Pathways of Proton Release in the Bacteriorhodopsin Photocycle†

László Zimányi,‡,§ György Váró,‖ Man Chang,⊥ Baofu Ni,⊥ Richard Needleman,⊥ and Janos K. Lanyi*,‡

Department of Physiology and Biophysics, University of California, Irvine, California 92717, Biological Research Center of the Hungarian Academy of Sciences, H-6701 Szeged, Hungary, and Department of Biochemistry, Wayne State University School of Medicine, Detroit, Michigan 48201

Received April 7, 1992; Revised Manuscript Received June 16, 1992

ABSTRACT: The pH dependencies of the rate constants in the photocycles of recombinant D96N and D115N/D96N bacteriorhodopsins were determined from time-resolved difference spectra between 70 ns and 420 ms after photoexcitation. The results were consistent with the model suggested earlier for proteins containing D96N substitution: BR $\xrightarrow{h\nu}$ K $\leftrightarrow$ L $\leftrightarrow$ M_1 $\leftrightarrow$ M_2 $\rightarrow$ BR. Only the $M_2 \rightarrow M_1$ back-reaction was pH-dependent: its rate increased with increasing $[H^+]$ between pH 5 and 8. We conclude from quantitative analysis of this pH dependency that its reverse, the $M_1 \rightarrow M_2$ reaction, is linked to the release of a proton from a group with a $pK_a = 5.8$. This suggests a model for wild-type bacteriorhodopsin in which at pH >5.8 the transported proton is released on the extracellular side from this as yet unknown group and on the 100-μs time scale, but at pH <5.8, the proton release occurs from another residue and later in the photocycle most likely directly from D85 during the O $\rightarrow$ BR reaction. We postulate, on the other hand, that proton uptake on the cytoplasmic side will be by D96 and during the N $\rightarrow$ O reaction regardless of pH. The proton kinetics as measured with indicator dyes confirmed the unique prediction of this model: at pH >6, proton release preceded proton uptake, but at pH <6, the release was delayed until after the uptake. The results indicated further that the overall $M_1 \rightarrow M_2$ reaction includes a second kinetic step in addition to proton release; this is probably the earlier postulated extracellular-to-cytoplasmic reorientation switch in the proton pump.

The broad outlines of the mechanism of light-driven proton transport in the retinal protein bacteriorhodopsin are now understood. The transport is based on proton transfers between the centrally located retinal Schiff base and aspartate residues in the two peripheral regions of this transmembrane protein, as well as proton release and uptake at the extracellular and the cytoplasmic aqueous interfaces [for recent reviews, cf. Mathies et al. (1991), Rothschild (1992), Oesterhelt et al. (1992), and Lanyi (1992)]. In the physiologically relevant pH range, the reaction cycle of the chromophore is described approximately by the suggested scheme: BR $\xrightarrow{h\nu}$ K $\leftrightarrow$ L $\leftrightarrow$ $M_1 \rightarrow M_2 \leftrightarrow$ N $\leftrightarrow$ O $\rightarrow$ BR (Váró & Lanyi, 1990a, 1991a; Gerwert et al., 1990a; Milder et al., 1991; Mathies et al., 1991). According to the predictions of the most recent structural model for the protein (Henderson et al., 1990), identification of the protonation state of buried aspartate residues by FTIR spectroscopy, and examination of the consequences of single-residue mutations [reviewed in Rothschild (1992) and Oesterhelt et al. (1992)], the step L $\leftrightarrow$ M in this scheme refers to proton exchange between the Schiff base and D85, while M $\leftrightarrow$ N refers to proton exchange between D96 and the Schiff base. These reactions move a proton effectively across nearly the entire transmembrane width of the protein because the overall process is given direction by the two reactions which appear to be unidirectional: $M_1 \rightarrow M_2$ and O $\rightarrow$ BR (Váró & Lanyi, 1991a,b). The former was suggested to be the switch which reorients the Schiff base from the extracellular to the cytoplasmic side and raises the pK_a of the Schiff base so as to change it from a proton donor to an acceptor (Váró & Lanyi, 1991a). The molecular nature of the switch is not yet known. It has been proposed to consist of rotation of the C_{14}–C_{15} single bond of the retinal (Gerwert & Siebert, 1986), but because of contrary evidence, others suggested a protein conformational change (Fodor et al., 1988a,b). A large decrease of entropy between proton release and uptake (Ort & Parson, 1979; Garty et al., 1982; Váró & Lanyi, 1991a), FTIR spectra (Engelhard et al., 1985; Gerwert et al., 1990b; Braiman et al., 1987; Ormos, 1991), dichroic measurements in the UV (Draheim & Cassim, 1985), resonance energy transfer between the retinal and a fluorophore at the aqueous interface (Hasselbacher & Dewey, 1986), and diffraction (Dencher et al., 1989; Nakasako et al., 1991; Koch et al., 1991) indicate that a protein conformational change does take place in the photocycle. That this change occurs while the Schiff base is deprotonated is indicated by the observations of Maeda and co-workers (Sasaki et al., 1992), who described the FTIR spectrum of a photoproduct of D96N bacteriorhodopsin, termed M_N, which had the chromophore skeletal bands of M but the changed protein bands of N. M_N was preceded by a normal M. Recently we found conditions where in D115N bacteriorhodopsin M_1 and M_2 are distinguished by a 15-nm difference in their absorption maxima (Váró et al., 1992). This shift might reflect a change in hydrogen bonding of the deprotonated Schiff base. The other unidirectional reaction, O $\rightarrow$ BR, has not been extensively studied; it is accompanied by retinal skeletal motions (Smith et al., 1983) as well as by reestablishment of the original deprotonated state of D85 (Siebert et al., 1982; Rothschild, 1992).

The $M_1 \rightarrow M_2$ and O $\rightarrow$ BR reactions have important energetic roles in the transport: they ensure that the reactions proceed in the forward direction. The free energy dissipated during these reactions in open purple membrane sheets (Váró

† This work was supported by grants from the National Institutes of Health (GM 29498) and the U.S. Department of Energy (DE-FGOER 13525).

* To whom correspondence should be addressed. Phone: (714) 856-7150. Fax: (714) 856-8540.

‡ University of California.

§ Permanent address: Biological Research Center of the Hungarian Academy of Sciences, Szeged, Hungary.

‖ Biological Research Center of the Hungarian Academy of Sciences.

⊥ Wayne State University School of Medicine.

0006-2960/92/0431-8535$03.00/0

& Lanyi, 1991a) will be conserved in closed systems (such as cells or cell envelope vesicles) as proton potential. In view of the simplicity of this pump, however, we have suspected that the two reactions are linked also mechanistically to proton transport. Exactly how the transported proton is released on the extracellular side is, in fact, not yet clear. Near pH 7 the proton is found to appear in the aqueous phase concurrently with deprotonation of the Schiff base (Drachev et al., 1984; Grzesiek & Dencher, 1986; Heberle & Dencher, 1990; Váró & Lanyi, 1990b), but at lower pH, the proton kinetics appear to be more complex (Dencher & Wilms, 1975; Váró & Lanyi, 1990b; Marinetti & Mauzerall, 1983). Linking the proton release to one of the chromophore reactions is complicated by the fact that many of the rate constants in this segment of the photocycle have similar values (Váró & Lanyi, 1991b); for example, what is observed as the L to M reaction should include the entire $L \rightarrow M_1 \rightarrow M_2$ sequence. Since FTIR has shown that D85 remains protonated until at least N (Gerwert et al., 1990; Braiman et al., 1991; Pfefferlé et al., 1991), and in fact until the $O \rightarrow BR$ reaction (Siebert et al., 1982; Rothschild, 1992), the proton must be released from another, so-far not identified group. We will refer to this group as XH.

In this report, we attempt to dissect the reactions at which proton is released into the extracellular medium. We describe how pH affects the first half of the photocycle kinetics in D96N and D115N/D96N bacteriorhodopsins between pH 4 and 8, and reevaluate our earlier measured (Váró & Lanyi, 1990b) proton kinetics. According to both kinds of measurements the pK_a of the unidentified proton release group XH drops during the photocycle to about 5.8. At pH >5.8, proton release is from XH and linked to the $M_1 \rightarrow M_2$ reaction, but at lower pH, it occurs increasingly during the $O \rightarrow BR$ reaction and therefore most likely directly from D85. Transport is compatible with either of the proton release pathways. In this extended model, the $M_1 \rightarrow M_2$ reaction is resolved into two sequential reactions: the proton release and a second kinetic component which is probably the switch step in the transport as earlier suggested.

MATERIALS AND METHODS

Preparation of purple membrane sheets, their handling, and the spectroscopy are described in previous papers [e.g., see Váró and Lanyi (1990b)]; the grid-search method of calculating the component spectra and the kinetics from measured time-resolved difference spectra will be published elsewhere.[1] In all experiments, the purple membranes were in 100 mM NaCl or KCl. When buffer was used, it was 50 mM phosphate. As before (Needleman et al., 1991), the optical multichannel spectroscopy was on purple membranes in acrylamide gels. The use of phenol red and chlorophenol red in measuring proton release and uptake kinetics in purple membrane suspensions was described before (Váró & Lanyi, 1990b). *Halobacterium halobium* strains carrying the gene with the single-residue substitution D96N (Asp96→Asn) and the double substitution D115N/D96N (Asp115→Asn *plus* Asp96→Asn) in bacteriorhodopsin were constructed by transformation with a halobacterial plasmid (Ni et al., 1990).

RESULTS

Kinetics of K, L, and M at Low pH. The group which releases the transported proton to the extracellular medium during the rise of M has not yet been identified, but by definition, it must have a high enough pK_a to be protonated initially, while during the photocycle its pK_a must decrease so the proton will be released. At a pH below the latter pK_a, the release of the proton will be ineffective because the group is kept in the protonated state by reprotonation from the surface aqueous layer, and the prerelease intermediate is thereby stabilized. In searching for the chromophore reaction associated with proton release, we have taken advantage of the fact that according to this argument the reaction linked to proton release will be identified by the pH dependency of its back-reaction. We searched, therefore, for a back-reaction in the first half of the photocycle whose rate would increase with proton concentration.

We described the photocycle between pH 4 and 8 by measuring time-resolved difference spectra for recombinant D96N and D115N/D96N bacteriorhodopsins. The D96N residue replacement allowed calculation of the component spectra and the kinetics with a grid-search method we have recently developed and will describe elsewhere.[1] This is because when the decay of M has a time constant >300 ms the N and O intermediates do not accumulate significantly and the calculation is simplified. For the D96N protein, this was the case at pH ≥4, and for D115N/D96N at pH ≥5. Perturbation of the first half of the photocycle by the D96N replacement is not likely to be great since the rate constants are not changed by more than 2-fold from wild-type (Váró & Lanyi, 1991b; Thorgeirsson et al., 1991). A possibly important role for D96 in proton transfer during the first half of the photocycle was suggested by FTIR spectra interpreted as deprotonation of D96 in the L intermediate (Braiman et al., 1988). However, according to recent data (Maeda et al., 1992), the FTIR features originate instead from changed hydrogen-bonding of this residue. The additional D115N residue replacement in the double mutant provided a useful alternative system because D115 affects the M_1 to M_2 reaction (Váró et al., 1992), and in preliminary experiments, we had found that the kinetics of L and M in D115N were noticeably pH-dependent. Figures 1 and 2 show measured difference spectra for these samples at pH 4 and 5. Comparison with spectra measured for D96N at pH 8 indicated[1] that the main difference at the lower pH was the shape of the spectra in the millisecond time range: the amplitude ratios of the positive maxima near 400 nm to the negative maxima near 570 nm approached about 0.61 in D96N at pH 8, but about 0.57 in D96N at pH 4 and about 0.52 in D115N/D96N at pH 5. Difference spectra as in Figures 1 and 2 were measured at various pH values up to pH 8 in both systems (not shown). To facilitate convenient signal-averaging, and to diminish the accumulation of M from the measuring light, the M decay time constant was kept near 300 ms at the higher pH values by adding various amounts of azide, which will function in this system as an external proton donor to the Schiff base and regulate the lifetime of M (Tittor et al., 1989; Otto et al., 1989; Cao et al., 1991). The rate constants in the first half of the photocycle were not affected by the azide. The derived spectra for K, L, and M under these conditions were very similar to those in D96N at higher pH (Váró & Lanyi, 1991b) except that the maximum of K in D115N/D96N was blue-shifted, to about 573 nm (not shown).

Figures 3 and 4 show the calculated kinetics of the intermediates (symbols) at pH 4, 6, and 7 in D96N and of pH 5, 6, and 7 in D115N/D96N bacteriorhodopsin under these conditions. The main effect of changing the pH will be on the decay of L. Unlike at pH 7, at lower pH the L intermediate persists beyond 1 ms and in increasing amounts (Alshuth &

[1] L. Zimányi and J. K. Lanyi, unpublished results.

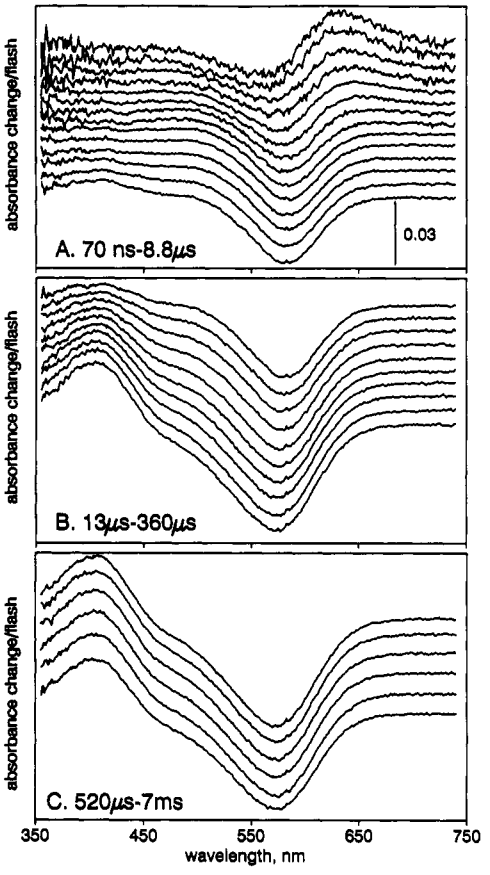

FIGURE 1: Time-resolved difference spectra for D96N bacteriorhodopsin at pH 4.0. Conditions: 100 mM NaCl, 50 mM phosphate, pH 4.0; 20 μM bacteriorhodopsin, 25 °C. Delay times after photoexcitation (beginning with the uppermost traces in each panel): (A) 70 ns, 100 ns, 210 ns, 310 ns, 450 ns, 650 ns, 940 ns, 1.4 μs, 2.9 μs, 4.2 μs, 6 μs, 8.8 μs; (B) 13, 18, 27, 39, 56, 81, 120, 170, 250, 360 μs; (C) 520 μs, 760 μs, 1.1 ms, 2.3 ms, 3.3 ms, 7 ms.

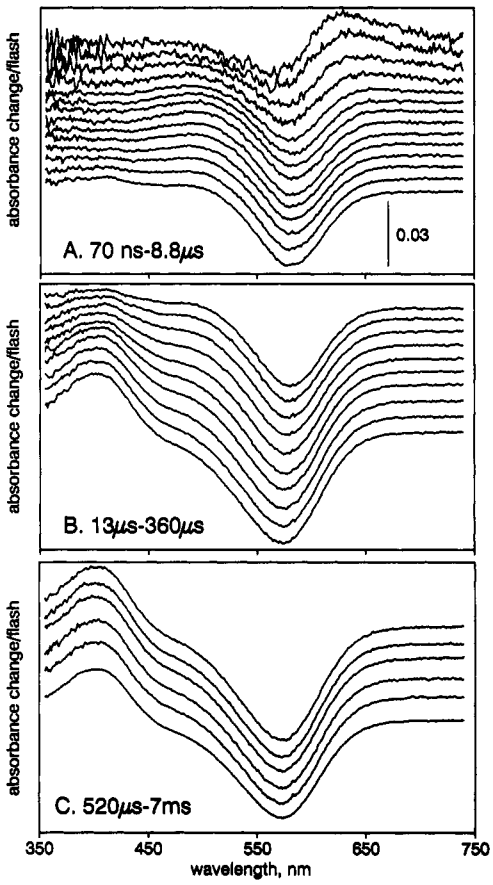

FIGURE 2: Time-resolved difference spectra for D115N/D96N bacteriorhodopsin at pH 5.0. Conditions: 100 mM NaCl, 50 mM phosphate, pH 5.0; 25 μM bacteriorhodopsin, 25 °C. Delay times after photoexcitation as in Figure 1.

Stockburger, 1986; Diller & Stockburger, 1988; Váró & Lanyi, 1991b). The data in Figures 3 and 4 confirm this: at lower pH, [L] does not approach zero as [M^{total}] reaches maximal values but coexists with the M state(s) in a roughly constant and pH-dependent concentration ratio until recovery of BR. The [L]/[M^{total}] ratio in this transient steady-state is particularly high in D115N/D96N bacteriorhodopsin. This change in the kinetics will have originated from the pH dependency of one or more rate constants in the photocycle. The data in Figures 3 and 4 were therefore evaluated in terms of the model K ↔ L ↔ M_1 ↔ M_2 → BR (lines), i.e., the earlier suggested scheme but including an M_2 to M_1 back-reaction. The model fit the points reasonably well.

In both samples, the calculated rates of the M_2 → M_1 back-reaction assumed significant values at lower pH; i.e., the M_1 → M_2 reaction was not unidirectional as at higher pH. Figure 5A,B shows the rate constants which gave the best fits. It is evident that in both systems the rate constants for the M_2 → M_1 back-reaction become greater with increasing [H^+]; this suggests that the rate is limited by proton uptake. No other rate constant between K and M_2 shows significant pH dependency. The main effect of the D115N residue replacement is a severalfold higher rate for the M_2 → M_1 back-reaction at each pH tested.

From these results and the arguments given above, it follows that the release of the transported proton is linked to the M_1 → M_2 forward reaction. This would be consistent with earlier results on the time scale on which the proton is released (Drachev et al., 1984; Grzesiek & Dencher, 1986; Heberle & Dencher, 1990; Váró & Lanyi, 1990b), but not with their interpretation which had associated it with the L → M reaction, thereby linking it directly to the protonation of D85. Such a revision requires that the M_1 → M_2 reaction be separated into two steps: in the first, a proton is exchanged between the unknown group XH and the extracellular aqueous phase (the proton release step), and in the second, whose existence we will argue below, access of the Schiff base changes from the extracellular to the cytoplasmic side (the "switch" step). The time-dependent concentrations of the intermediates in Figures 3 and 4 (symbols) were therefore evaluated in terms of the following reaction sequence: L ↔ M_1 ↔ M_1' + H^+ ↔ M_2', where M_1 ↔ M_1' + H^+ is the protonation equilibrium between the proton release group XH and the aqueous phase and M_1' ↔ M_2' is the switch. The superscript prime denotes those states in which XH is deprotonated. This sequence by itself is untenable, however, because it predicts that at pH values low enough to observe significant M_2 → M_1 back-reaction the overall M decay will be slowed by stabilization of M_1. In fact, the M decay is not slowed at pH as low as 3.5 in wild-type bacteriorhodopsin (Váró & Lanyi, 1989). Neither is transport inhibited at low pH, provided that blue membrane is not formed, i.e., at pH as low as 4–5 (Ormos et al., 1985; Kouyama & Nasuda-Kouyama, 1989; Váró et al., 1990). For these reasons, the direct reaction M_1 ↔ M_2, in which deprotonation of XH does not take place, was retained in the model. Thus, from the point of view of proton release, there are two alternatives (Figure 6): a high pH pathway in which the transported proton is released from XH and a low-pH pathway in which XH remains protonated and the proton is released later in the cycle. In Figure 6, these two pathways are described

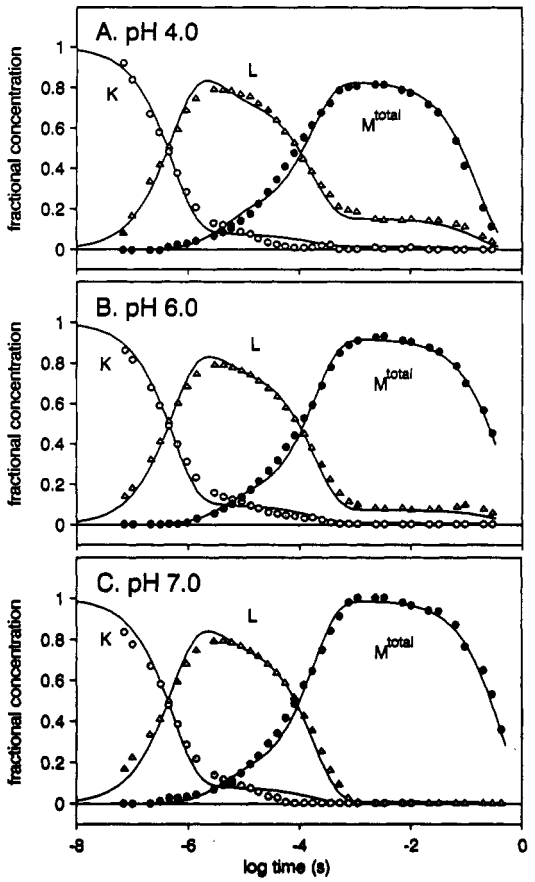

FIGURE 3: Kinetics of the photointermediates of D96N bacteriorhodopsin at pH 4.0 (A), 6.0 (B), and 7.0 (C). Conditions as in Figure 1, but at pH 6.0 20 μM and at pH 7.0 200 μM NaN_3 were added. The symbols are the calculated concentrations of K (○), L (△), and M^{total} (●), as functions of delay time after photoexcitation. The lines are the best fits of the model $K \leftrightarrow L \leftrightarrow M_1 \leftrightarrow M_2 \rightarrow BR$.

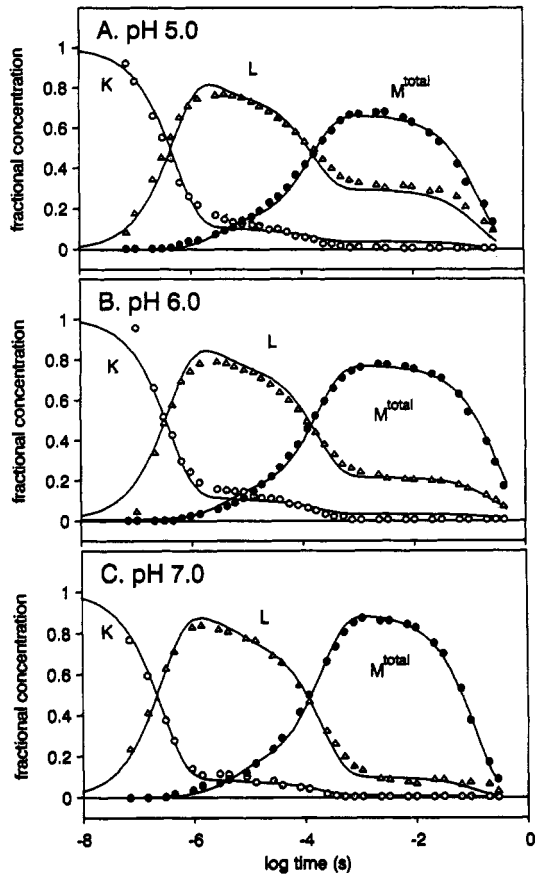

FIGURE 4: Kinetics of the photointermediates of D115N/D96N bacteriorhodopsin at pH 5.0 (A), 6.0 (B), and 7.0 (C). Conditions as in Figure 2, but at pH 6.0 20 μM and at pH 7.0 200 μM NaN_3 were added. The symbols are the calculated concentrations of K (○), L (△), and M^{total} (●), as functions of delay time after photoexcitation. The lines are the best fits of the model $K \leftrightarrow L \leftrightarrow M_1 \leftrightarrow M_2 \rightarrow BR$.

for the wild-type protein as $M_1 \leftrightarrow M_1' \leftrightarrow M_2' \leftrightarrow N' \leftrightarrow O' \rightarrow BR$ and as $M_1 \leftrightarrow M_2 \leftrightarrow N \leftrightarrow O \rightarrow BR$, where M_2, N, and O are analogous to M_2', N', and O' but designate states in which the proton release group XH remains protonated. Other features of this model will be discussed below.

Kinetic analyses of the time-dependent concentrations of L and the measured sum of M states (as in Figures 3 and 4) cannot resolve the rates of reactions among the proposed multiple M substates. However, the equilibrium constants of the additional reactions can be calculated from the pH dependency of the ratio of the observed concentration of L to the sum of the concentrations of all M states because late in the photocycle a quasi-steady-state will have developed among these intermediates (Figures 3 and 4). The concentration ratio in this steady state will be

$$\frac{[L]}{[M^{total}]} = \frac{K_1}{1 + K_2 + K_3/[H^+] + K_2K_3/[H^+]} \quad (1)$$

where $[M^{total}] = [M_1] + [M_1'] + [M_2] + [M_2']$, $K_1 = k_{LM1}/k_{M1L}$, $K_2 = [M_2']/[M_1'] = [M_2]/[M_1]$, and $K_3 = [M_1'][H^+]/[M_1]$. K_1 has the same meaning as in the model used in Figure 5A,B. It is pH-independent, and its average value is 4 for D96N and 5 for D115N/D96N between pH 4 and 8. In the extended model (Figure 6), K_2 becomes the unknown equilibrium constant for the switch reaction, assumed to be the same in the two pathways. K_3 is the unknown equilibrium constant for the protonation of XH. K_2 and K_3 will be fully determined by the pH dependency of $[L]/[M^{total}]$ and its limiting value at pH $\ll pK_a$. Panels A and B of Figure 7 show

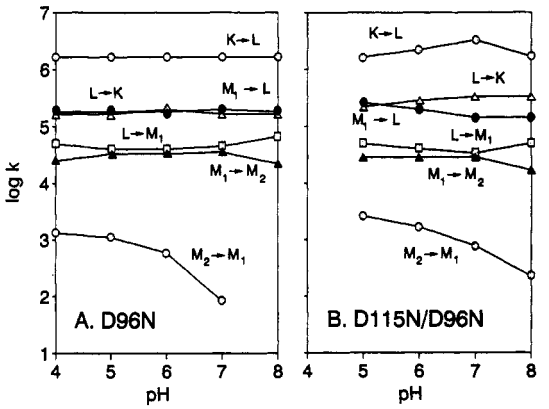

FIGURE 5: Dependency of the photocycle rate constants on pH. The values were from fits to time-dependent concentrations as in Figures 3 and 4. (A) D96N bacteriorhodopsin; (B) D115N/D96N bacteriorhodopsin. In D96N, the rate constant for the $M_2 \rightarrow M_1$ back-reaction at pH ≥7 was below detection; the point shown is the highest value allowed by conservative fitting, given the noise in the data. (○) k_{KL}; (△) k_{LK}; (□) k_{LM1}; (●) k_{M1L}; (▲) k_{M1M2}; (◇) k_{M2M1}.

the observed $[L]/[M^{total}]$ as functions of pH in D96N and D115N/D96N, respectively (symbols), calculated as the average of the ratio of the fractional concentrations of L and M between 5 and 50 ms in the kinetics (cf. Figures 3 and 4, symbols). The lines are the best fits of eq 1. The data define K_2 as 21 and 7 in D96N and D115N/D96N, respectively, and K_3 as 1.58×10^{-6} M. The pK_a of the proton release group XH is therefore 5.8 in both samples. It refers to bulk rather than surface pH; the actual pK_a will be somewhat lower.

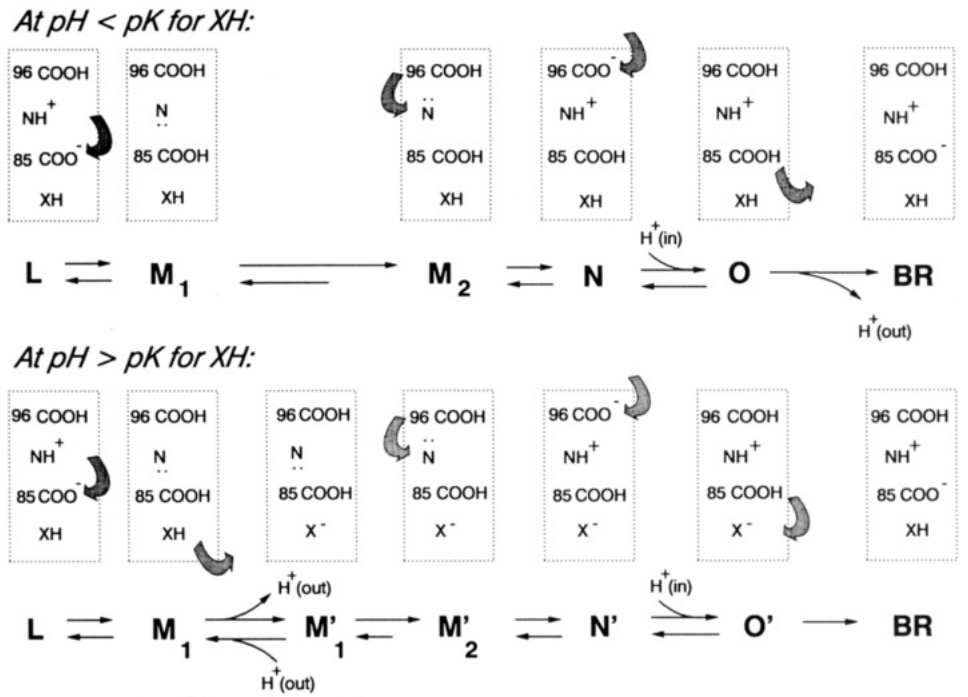

FIGURE 6: Suggested model for the photocycle in wild-type bacteriorhodopsin which takes into account the protonation state of the extracellular proton release group XH. D96 on the cytoplasmic side, the retinal Schiff base, and D85 and XH on the extracellular side are shown schematically as 96 COOH, NH^+, and 85 COO^-, XH, respectively. Proton transfers inside the protein and at the aqueous interfaces are shown with shaded arrows; observable proton release and uptake in the medium on the extracellular (out) and cytoplasmic (in) sides are as indicated in the reaction sequences.

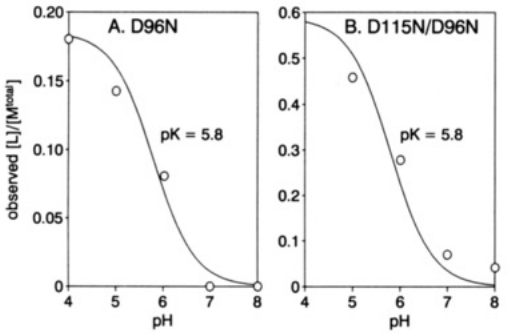

FIGURE 7: Calculation of the reaction equilibria for the M substates proposed in Figure 6. (A) D96N bacteriorhodopsin; (B) D115N/D96N bacteriorhodopsin. The equilibrium constants of the M substates were calculated from the pH dependencies of the ratio of [L] to $[M^{total}]$ during the steady-state which develops (cf. Figures 3 and 4, symbols), using eq 1 as described in the text. The calculated value for K_2 for D96N is 21, and for D115N/D96N 7; the pK_a of XH (=$-\log K_3$) is 5.8 in both samples.

Without M_2 and M_2' (i.e., in a simpler model where the earlier described M_2 state is identical to what we now designate as M_1') at pH $\ll$5.8, the limiting $[L]/[M^{total}]$ equilibrium ratio should approach the values expected from the $[L]/[M_1]$ equilibrium ratio, which is 4 in D96N and 5 in D115N/D96N, rather than the observed values which are about 0.2 and 0.6 (Figure 7A,B). Thus, the inclusion of the second kinetic component in the overall M_1 to M_2 reaction is justified. Although shown in Figure 6 as equilibration, it is an equilibrium which lies strongly in the forward direction.

pH Dependency of Proton Release and Uptake. The model in Figure 6 has unique predictions for the pH dependency of the proton kinetics. At pH $\gg$ pK_a for XH, the photocycle will be mostly via the high-pH pathway, where, as suggested in many reports, proton release on the extracellular side is *before* proton uptake on the cytoplasmic side. At pH $\ll$ pK_a, however, most of the photocycle will pass via the low-pH pathway, where we postulate that the proton is released directly to the aqueous phase only when D85 deprotonates during the O $\rightarrow$ BR reaction. On the other hand, there is no reason to suppose that proton uptake on the cytoplasmic surface is not during the N $\leftrightarrow$ O and the analogous N' $\leftrightarrow$ O' reaction, i.e., by D96 (Gerwert et al., 1989; Otto et al., 1989; Butt et al., 1989), whatever the protonation state of XH. Thus, in this pathway, the proton is released on the extracellular side *after* proton uptake on the cytoplasmic side. At pH = pK_a, proton release will be divided equally between the two alternatives. The expected kinetics of the protons, normalized to the amount of chromophore photocycling, are therefore

$$[H^+]_t \text{ (at pH} \gg pK_a) = -\exp(-t/\tau_1) + \exp(-t/\tau_2) \quad (2)$$

$$[H^+]_t \text{ (at pH} \ll pK_a) = -\exp(-t/\tau_3) + \exp(-t/\tau_2) \quad (3)$$

where τ_1, τ_2, and τ_3 are the relaxation times of extracellular proton release from XH (during $M_1 \leftrightarrow M_1'$), cytoplasmic proton uptake by D96 (during N $\rightarrow$ O), and extracellular proton release from D85 (during O $\rightarrow$ BR), respectively. At high pH, therefore, the protein shows *net proton deficit* during the photocycle. This occurs while M_1' and M_2' *plus* N' are present (at pH 7, this is roughly equivalent to M^{total}). At low pH, in contrast, there will be *net proton gain* by the protein, at the time when O is present. Residue replacements which eliminate XH as a proton release group will have the same effect on the proton kinetics as lowering the pH for wild-type protein. The single time constant τ_1 ignores the expected multiexponential kinetics for the proton release from XH, but this process was not resolved in any case because the time response of the dye had limited the measurements. At pH values between these extremes, a mixture of these kinetics will appear, weighted in proportion of the two pathways. The expected release and uptake proton kinetics, and their algebraic sum, i.e., the net protonation state of the protein, are shown in Figure 8. The prediction for the latter (dashed line) is a set of complex and nontrivial pH-dependent curves.

As several others (Drachev et al., 1984; Grzesiek &

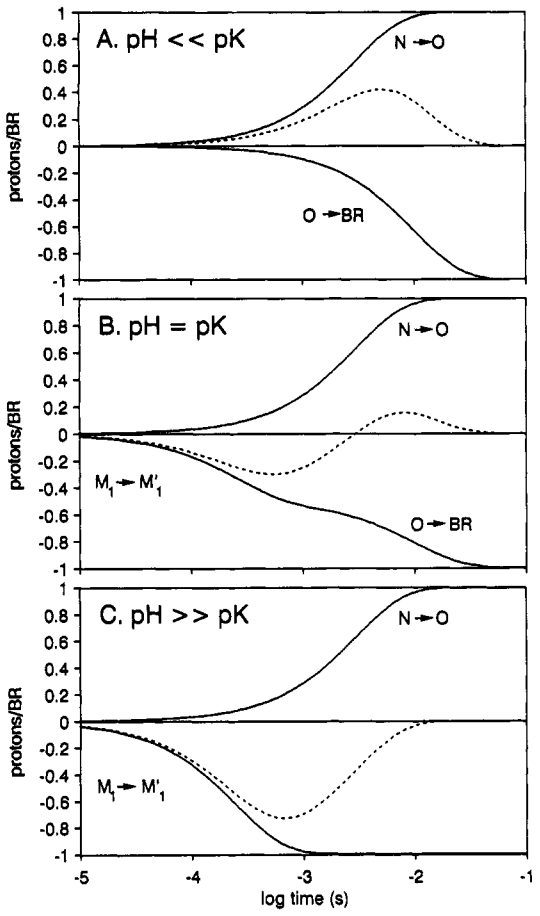

FIGURE 8: Expected proton kinetics according to the model in Figure 6. In which reaction proton is released on the extracellular side during transport is dependent on the pH, but the uptake of the proton on the cytoplasmic side is in the N → O reaction regardless of the pH. At a pH well below the pK_a of the proton release group XH, proton release is in the O → BR reaction (A), and at a pH well above the pK_a, proton release is in the $M_1 \rightarrow M_1'$ reaction (C), as described by eq 2 and 3. At pH = pK_a, the fraction of proton released is equally divided between the two alternatives (B). The dashed lines are the weighted algebraic sums of the release and uptake kinetics and represent the expected time-resolved net protonation state of bacteriorhodopsin. The time constants used in this simulation are 250 μs for the $M_1 \rightarrow M_1'$ reaction (i.e., not the actual time constant but what appears to be the rate the dye follows pH changes), 3 ms for the N → O reaction, and 10 ms for the O → BR reaction.

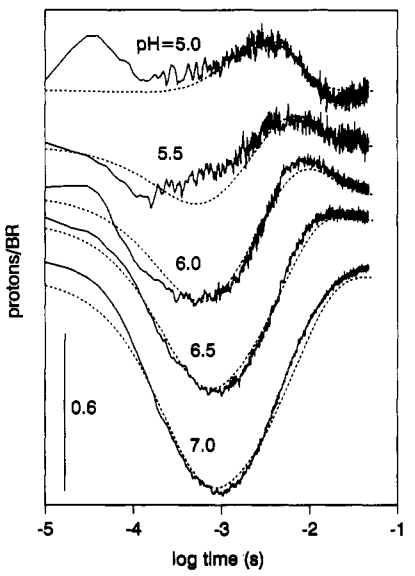

FIGURE 9: Proton kinetics after photoexcitation, as measured with phenol red and chlorophenol red, and their fits with the predictions of the model (cf. Figures 6 and 8). The solid lines are data from Váró and Lanyi (1990b), at pH 5, 5.5, 6, 6.5, and 7 (in 100 mM KCl) as indicated. The dashed lines are the model using the following phenomenological time constants (at pH 5, 5.5, 6, 6.5, and 7, respectively): 2, 3, 3, 5, and 7 ms for the N → O reaction and 4, 7, 11, and 13 ms for the O → BR reaction. At pH 7, the latter made no contribution to the model. For the $M_1 \rightarrow M_1'$ reaction, the data are limited by the time response of the dye which is estimated to be 250 μs under these conditions.

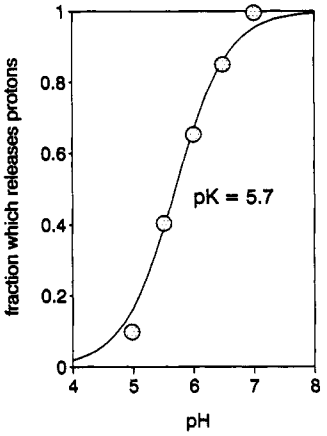

FIGURE 10: pK_a of the proton release group XH, as calculated from the pH dependency of the dye-detected proton kinetics in Figure 9. The pK_a is directly estimated from the fraction of photoexcited bacteriorhodopsin which proceeds via the pathway containing deprotonated XH, i.e., the fraction of the pathway described by eq 2. The pK_a by this method is 5.7.

Dencher, 1986; Otto et al., 1989; Herberle & Dencher, 1990), we had earlier described the appearance and disappearance of protons in the aqueous phase during the photocycle, but with phenol red and chlorophenol red as indicators which allowed studying the proton kinetics over a pH range between pH 5 and 9 (Váró & Lanyi, 1990b). The predictions of the model were tested by reevaluating these proton kinetics in wild-type bacteriorhodopsin. As shown in Figure 9, the data between pH 5 and 7 are described remarkably well by eq 2 and 3; the major discrepancies are at early times where there are few data points. The time constant τ_1 refers here to the rate at which the dye responds to proton release; τ_2 and τ_3 correspond reasonably well to the time constants of the N → O and O → BR reactions, respectively (Váró & Lanyi, 1990b). The proportion of the two pathways is expected to follow roughly the protonation state of the proton release group XH. The pH dependency of bacteriorhodopsin fraction which releases a proton indicates that XH has a pK_a of 5.7 (Figure 10). The good agreement of this value, calculated solely from the dye data, with the pK_a calculated solely from the spectroscopic data (Figure 7A,B) is strong evidence in favor of the model in Figure 6.

It should be mentioned that according to earlier reports the chromophore absorption was strongly altered in D115N bacteriorhodopsin (Mogi et al., 1988; Stern et al., 1989; Subramaniam et al., 1990) and proton uptake preceded proton release at pH 6 (Marinetti et al., 1989), suggesting that replacement of D115 causes significant perturbation of the protein and the transport process. These results are inconsistent with the wild-type-like absorption spectrum of D115N (Váró et al., 1992), and the near-normal kinetics in the first half of the photocycle of D115N/D96N (Figures 4 and 5B). Additionally, the reported reversal of the protonation order is inconsistent with our observation[2] that above pH 5 there

is net proton release during illumination of D115N bacteriorhodopsin. The reason for these differences is most likely the fact that the earlier reports were with *Escherichia coli* expressed bacteriorhodopsin while our results are with proteins from an halobacterial expression system; significant differences between products of the two expression systems exist in the case of at least one other residue replacement (Needleman et al., 1991).

DISCUSSION

We have identified the only pH-dependent process in the first half of the bacteriorhodopsin photocycle between pH 4 and 8. It is the $M_2 \rightarrow M_1$ back-reaction in our previously proposed scheme; because its rate increases with $[H^+]$, we suggest that it is limited by proton uptake. We argue from this result that its reverse, the $M_1 \rightarrow M_2$ forward reaction, is accompanied by proton release. Thus, even though the first phase of the proton transport, i.e., proton release of the extracellular side, coincides in time with the overall rise of the M intermediate, we link it not to the L to M step but to a reaction between M substates.

Two modifications of the photocycle scheme follow from this finding (Figure 6). (1) The $M_1 \rightarrow M_2$ reaction is resolved into two steps in series: deprotonation ($M_1 \leftrightarrow M_1' + H^+$) and switch ($M_1' \leftrightarrow M_2'$). Proton release in the former is from the unidentified residue XH on the extracellular side. The data indicate that the pK_a of XH becomes about 5.8 in the M_1 state (Figures 7 and 10). At pH well above this value, the overall $M_1 \rightarrow M_2$ reaction appears unidirectional, but at lower pH, there is measurable back-reaction (Figure 5). The $M_1 \rightarrow M_1' + H^+ \leftrightarrow M_2' \leftrightarrow N' \leftrightarrow O' \rightarrow$ BR sequence, which would be a minor modification of the earlier model (Váró & Lanyi, 1991a), therefore applies strictly only to the kinetics at pH well above 5.8. (2) At pH below 5.8, the products of M_1 decay will be M_2, N, and O states in which XH remains protonated. In this low-pH pathway, the proton release is during the $O \rightarrow$ BR step.

The existence of an alternative pathway in which proton release is delayed until the last step in the photocycle is confirmed by the dramatic reversal in the proton kinetics at lower pH, as measured with phenol red and chlorophenol red (Figure 9). Net proton gain by the protein roughly concurrent with the accumulation of O, i.e., uptake at about 3 ms followed by release at about 10 ms at pH <5 (as in Figure 9), had been found before with bromcresol green (Dencher & Wilms, 1975) and with conductance measurements (Marinetti & Mauzerall, 1983). In the latter case, the ion responsible for the transient conductance decrease was identified as a proton from changes of the magnitude and sign of the measured effect upon adding an anionic buffer. A simpler experiment is the measurement of pH changes in the medium with a glass electrode in photostationary states containing mainly M, N, and O as photoproducts during constant illumination. Several reports (Garty et al., 1977; Fischer & Oesterhelt, 1980; Takeuchi et al., 1981; Váró & Lanyi, 1990b) agree that in such experiments there is net *proton loss* from the purple membrane sheets at ca. pH >5 but net *proton gain* at ca. pH <5, in amounts consistent with what would be expected for the accumulation of the late photocycle intermediates. Raising the temperature shifted the photostationary state strongly toward increasing proton gain, reversing the direction of the net pH change at intermediate pH (Garty et al., 1977). This links the proton gain to the O intermediate, because the ratio of [O] to [M *plus* N] in the photostationary state increases dramatically as the temperature is increased.[2] However, in another time-resolved study with bromcresol green and dinitrophenol (Mitchell & Rayfield, 1986), only proton release was detected between about 150 μs and the end of all absorbance changes in the photocycle (about 100 ms under the conditions used) at pH between 4 and 5. The reason for this disagreement is not clear. It would seem that the observed net proton uptake at low pH during steady-state illumination requires that time-resolved measurements show net proton uptake *at some time* during the photocycle.

In view of the results, a more complicated model for the photocycle seems unavoidable. The pH dependencies of the kinetics of the intermediates and of the pattern of the appearance and disappearance of the proton in the medium strongly suggest that the pK_a of the proton release group XH is in the physiological pH range and this will necessarily lead to models in which the pump can function effectively at pH both above and below this pK_a. We suggest the scheme in Figure 6 because it is supported independently by transient spectroscopy and dye kinetics. The details of this solution of the problem require a few additional comments. (1) We have retained the idea of a switch reaction in addition to the deprotonation reaction within the overall M_1 to M_2 transition, partially because it is conceptually required for the transport, but also because the data indicate the need for the additional step. The existence of M_2, as kinetically distinct from M_1 in the low-pH pathway, is required by the discrepancy between the expected and found limiting $[L]/[M^{total}]$ ratio (Figure 7). Interestingly, but for reasons not yet clear, it is solely this switch step which is affected by the D115N residue replacement. (2) We have placed the deprotonation before the switch reaction, rather than after, implying thereby that the deprotonation of XH occurs while the Schiff base is in its preswitch arrangement. All of the data in this report are, in fact, consistent with either this alternative or another in which the postswitch arrangement of the Schiff base is a prerequisite of the deprotonation of XH. In the latter version, the model in Figure 6 would not contain M_1' but a protonation equilibrium between M_2 and M_2'. The third possibility is that the deprotonation of XH and the switch are independent of one another, and a protonation equilibrium exists also between M_2 and M_2'. The calculations and the predictions of the model for the proton kinetics are little affected by the choice among these alternatives. (3) In the low-pH pathway in Figure 6, we show the proton as released into the medium during the $O \rightarrow$ BR reaction directly from D85 rather than through a more complex mechanism. There is no evidence for this simplifying assumption, and it is not an essential part of the model. A recent report on the stabilization of the O intermediate in Y185F bacteriorhodopsin suggests the possible involvement of Y185 in the deprotonation of D85 (Sonar et al., 1992).

We wish to emphasize that the alternative pathways in Figure 6 are really aspects of a single photocycle, as they reflect simply the idea that events on the cytoplasmic side of the protein (protonation changes of D96) may proceed independently of events on the extracellular side (protonation changes of D85 and XH). Thus, if the $M_1 \leftrightarrow M_1' \leftrightarrow M_2' \leftrightarrow N' \leftrightarrow O' \rightarrow$ BR sequence has the same rate constants as the $M_1 \leftrightarrow M_2 \leftrightarrow N \leftrightarrow O \rightarrow$ BR sequence and the intermediates have similar spectra in the visible, as appears to be the case, spectroscopic measurements of the M to BR segment of the photocycle will not reveal the existence of a branch at M_1. From this point of view, the chromophore reactions are

[2] Y. Cao and J. K. Lanyi, unpublished results.

represented accurately by the single-cycle scheme we suggested earlier (Váró & Lanyi, 1991a), even though a complete description of the chromophore *plus* protein reactions has to include also the pH-dependent protonation state of the proton release group XH.

There are some clues to the identity of XH. Of the four known protonated groups in bacteriorhodopsin, D115 is not a candidate (cf. this work and our finding[2] that proton release from D115N is like wild-type). Y185 and Y57 or other tyrosines are unlikely because recent time-resolved UV absorption (Sharonov et al., 1991) and UV-Raman spectra (Ames et al., 1992) rule out the deprotonation of any tyrosine during the photocycle. R82 which had been suggested as the proton release group (Mathies et al., 1991) seems somewhat unlikely because a pK_a of 6 for a guanidinium group is unprecedented in proteins. On the other hand, a water molecule bound to R82 (Rothschild et al., 1992) is a possible candidate. In any case, R82 seems to be required for early proton release. Dye kinetics indicated that in R82A bacteriorhodopsin the usual proton release roughly concurrent with M near pH 7 was replaced by delayed proton uptake coincident with absorption increase at 650 nm, i.e., the O state (Otto et al., 1990), much in the same way as it occurs in wild-type at pH 5 (Figure 9).

The scheme in Figure 6 provides the rationale for direct mechanistic roles of both the $M_1 \rightarrow M_2$ and $O \rightarrow BR$ reactions in the creation of protonmotive force during transport. Their thermodynamic descriptions are therefore all the more interesting. The energetics of the overall M_1 to M_2 transition were characterized earlier as dissipation of free energy, which made this reaction virtually unidirectional and conversion of enthalpy to entropy (Váró & Lanyi, 1991a). The ΔG is now resolved into a pH-independent component, $\Delta G_{M1M2} = \Delta G_{M1'M2'} = -RT \log K_2$, and a pH-dependent component which relates directly to the difference between the pK_a of XH and the pH, $\Delta G_{M1M1'} = -RT \log (K_3/[H^+])$. The former amounts to about 7.5 kJ/mol in D96N and about 4.8 kJ/mol in D115N/D96N, and we assume it represents free energy dissipation at the switch step. We attribute, therefore, the unidirectionality of the overall $M_1 \rightarrow M_2$ reaction partly to the switch step which leads to an equilibrium strongly biased in the forward direction, and partly to the proton release whenever the pH is higher than the pK_a of XH. The detailed enthalpy and entropy changes in the proposed extended reaction scheme for the M substates in Figure 6 will be subjects of our future investigations. As to the energetics of the $O \rightarrow BR$ step, it was surmised only that at least 20 J/mol of free energy is dissipated here, mostly as $T\Delta S$ (Váró & Lanyi, 1991a). In BR, the pK_a of D85 is about 2.5; this is low enough to release the proton either to the aqueous phase or to X^- with a sizable negative contribution to ΔG at any physiological pH.

REFERENCES

Alshuth, T., & Stockburger, M. (1986) *Photochem. Photobiol. 43*, 55–66.

Ames, J. B., Raap, J., Lugtenburg, J., & Mathies, R. A. (1992) *Biophys. J. 61*, A533.

Braiman, M. S., Ahl, P. L., & Rothschild, K. J. (1987) *Proc. Natl. Acad. Sci. U.S.A. 84*, 5221–5225.

Braiman, M. S., Mogi, T., Marti, T., Stern, L. J., Khorana, H. G., & Rothschild, K. J. (1988) *Biochemistry 27*, 8516–8520.

Braiman, M. S., Bousché, O., & Rothschild, K. J. (1991) *Proc. Natl. Acad. Sci. U.S.A. 88*, 2388–2392.

Butt, H.-J., Fendler, K., Bamberg, E., Tittor, J., & Oesterhelt, D. (1989) *EMBO J. 8*, 1657–1663.

Cao, Y., Váró, G., Chang, M., Ni, B., Needleman, R., & Lanyi, J. K. (1991) *Biochemistry 30*, 10972–10979.

Dencher, N. A., & Wilms, M. (1975) *Biophys. Struct. Mech. 1*, 259–271.

Dencher, N. A., Dresselhaus, D., Zaccai, G., & Büldt, G. (1989) *Proc. Natl. Acad. Sci. U.S.A. 86*, 7876–7879.

Diller, R., & Stockburger, M. (1988) *Biochemistry 27*, 7641–7651.

Drachev, L. A., Kaulen, A. D., & Skulachev, V. P. (1984) *FEBS Lett. 178*, 331–335.

Draheim, J. E., & Cassim, J. Y. (1985) *Biophys. J. 47*, 497–507.

Engelhard, M., Gerwert, K., Hess, B., Kreutz, W., & Siebert, F. (1985) *Biochemistry 24*, 400–407.

Fischer, U. C., & Oesterhelt, D. (1980) *Biophys. J. 31*, 139–145.

Fodor, S. P., Pollard, W. T., Gebhard, R., van den Berg, E. M., Lugtenburg, J., & Mathies, R. A. (1988a) *Proc. Natl. Acad. Sci. U.S.A. 85*, 2156–2160.

Fodor, S. P., Ames, J. B., Gebhard, R., van der Berg, E. M., Stoeckenius, W., Lugtenburg, J., & Mathies, R. A. (1988b) *Biochemistry 27*, 7097–7101.

Garty, H., Klemperer, G., Eisenbach, M., & Caplan, S. R. (1977) *FEBS Lett. 81*, 238–242.

Garty, H., Caplan, S. R., & Cahen, D. (1982) *Biophys. J. 37*, 405–415.

Gerwert, K., & Siebert, F. (1986) *EMBO J. 5*, 805–811.

Gerwert, K., Hess, B., Soppa, J., & Oesterhelt, D. (1989) *Proc. Natl. Acad. Sci. U.S.A. 86*, 4943–4947.

Gerwert, K., Souvignier, G., & Hess, B. (1990a) *Proc. Natl. Acad. Sci. U.S.A. 87*, 9774–9778.

Gerwert, K., Hess, B., & Engelhard, M. (1990b) *FEBS Lett. 261*, 449–454.

Grzesiek, S., & Dencher, N. A. (1986) *FEBS Lett. 208*, 337–342.

Hasselbacher, C. A., & Dewey, T. G. (1986) *Biochemistry 25*, 6236–6243.

Heberle, J., & Dencher, N. A. (1990) *FEBS Lett. 277*, 277–280.

Henderson, R., Baldwin, J. M., Ceska, T. A., Zemlin, F., Beckmann, E., & Downing, K. H. (1990) *J. Mol. Biol. 213*, 899–929.

Koch, M. H. J., Dencher, N. A., Oesterhelt, D., Plöhn, H.-J., Rapp, G., & Büldt, G. (1991) *EMBO J. 10*, 521–526.

Kouyama, T., & Nasuda-Kouyama, A. (1989) *Biochemistry 28*, 5963–5970.

Lanyi, J. K. (1992) *J. Bioenerg. Biomembr. 24*, 169–179.

Maeda, A., Sasaki, J., Shichida, Y., Yoshizawa, T., Chang, M., Ni, B., Needleman, R., & Lanyi, J. K. (1992) *Biochemistry 31*, 4684–4690.

Marinetti, T., & Mauzerall, D. (1983) *Proc. Natl. Acad. Sci. U.S.A. 80*, 178–180.

Marinetti, T., Subramaniam, S., Mogi, T., Marti, T., & Khorana, H. G. (1989) *Proc. Natl. Acad. Sci. U.S.A. 86*, 529–533.

Mathies, R. A., Lin, S. W., Ames, J. B., & Pollard, W. T. (1991) *Annu. Rev. Biophys. Biophys. Chem. 20*, 491–518.

Milder, S. J., Thorgeirsson, T. E., Miercke, L. J. W., Stroud, R. M., & Kliger, D. S. (1991) *Biochemistry 30*, 1751–1761.

Mitchell, D., & Rayfield, G. W. (1986) *Biophys. J. 49*, 563–566.

Mogi, T., Stern, L. J., Marti, T., Chao, B. H., & Khorana, H. G. (1988) *Proc. Natl. Acad. Sci. U.S.A. 85*, 4148–4152.

Nakasako, M., Kataoka, M., Amemiya, Y., & Tokunaga, F. (1991) *FEBS Lett. 292*, 73–75.

Needleman, R., Chang, M., Ni, B., Váró, G., Fornes, J., White, S. H., & Lanyi, J. K. (1991) *J. Biol. Chem. 266*, 11478–11484.

Ni, B., Chang, M., Duschl, A., Lanyi, J. K., & Needleman, R. (1990) *Gene 90*, 169–172.

Oesterhelt, D., Tittor, J., & Bamberg, E. (1992) *J. Bioenerg. Biomembr. 24*, 181–191.

Ormos, P. (1991) *Proc. Natl. Acad. Sci. U.S.A. 88*, 473–477.

Ormos, P., Hristova, S. G., & Keszthelyi, L. (1985) *Biochim. Biophys. Acta 809*, 181–186.

Ort, D. R., & Parson, W. W. (1979) *Biophys. J. 25*, 355–364.

Otto, H., Marti, T., Holz, M., Mogi, T., Lindau, M., Khorana, H. G., & Heyn, M. P. (1989) *Proc. Natl. Acad. Sci. U.S.A. 86*, 9228–9232.

Otto, H., Marti, T., Holz, M., Mogi, T., Stern, L. J., Engel, F., Khorana, H. G., & Heyn, M. P. (1990) *Proc. Natl. Acad. Sci. U.S.A. 87*, 1018–1022.
Pfefferlé, J.-M., Maeda, A., Sasaki, J., & Yoshizawa, T. (1991) *Biochemistry 30*, 6548–6556.
Rothschild, K. J. (1992) *J. Bioenerg. Biomembr. 24*, 147–167.
Rothschild, K. J., He, Y.-W., Sonar, S., Marti, T., & Gobind Khorana, H. (1992) *J. Biol. Chem. 267*, 1615–1622.
Sasaki, J., Shichida, Y., Lanyi, J. K., & Maeda, A. (1992) *J. Biol. Chem.* (in press).
Sharanov, A. Yu., Tkachenko, N. V., Savransky, V. V., & Dioumaev, A. K. (1991) *Photochem. Photobiol. 54*, 889–895.
Siebert, F., Mantele, W., & Kreutz, W. (1982) *FEBS Lett. 141*, 82–87.
Smith, S. O., Pardoen, J. A., Mulder, P. P. J., Curry, B., Lugtenburg, J., & Mathies, R. A. (1983) *Biochemistry 22*, 6141–6148.
Sonar, S. M., Bouché, O., He, Y.-W., Rath, P., Khorana, H. G., & Rothschild, K. J. (1992) *Biophys. J. 61*, A531.
Stern, L. J., Ahl, P. L., Marti, T., Mogi, T., Duñach, M., Berkovitz, S., Rothschild, K. J., & Khorana, H. G. (1989) *Biochemistry 28*, 10035–10042.
Subramaniam, S., Marti, T., & Khorana, H. G. (1990) *Proc. Natl. Acad. Sci. U.S.A. 87*, 1013–1017.
Takeuchi, Y., Ohno, K., Yoshida, M., & Nagano, K. (1981) *Photochem. Photobiol. 33*, 587–592.
Thorgeirsson, T. E., Milder, S. J., Miercke, L. J. W., Betlach, M. C., Shand, R. F., Stroud, R. M., & Kliger, D. S. (1991) *Biochemistry 30*, 9133–9142.
Tittor, J., Soell, C., Oesterhelt, D., Butt, H.-J., & Bamberg, E. (1989) *EMBO J. 8*, 3477–3482.
Váró, G., & Lanyi, J. K. (1989) *Biophys. J. 56*, 1143–1151.
Váró, G., & Lanyi, J. K. (1990a) *Biochemistry 29*, 2241–2250.
Váró, G., & Lanyi, J. K. (1990b) *Biochemistry 29*, 6858–6865.
Váró, G., & Lanyi, J. K. (1991a) *Biochemistry 30*, 5016–5022.
Váró, G., & Lanyi, J. K. (1991b) *Biochemistry 30*, 5008–5015.
Váró, G., Duschl, A., & Lanyi, J. K. (1990) *Biochemistry 29*, 3798–3804.
Váró, G., Zimányi, L., Chang, M., Ni, B., Needleman, R., & Lanyi, J. K. (1992) *Biophys. J. 61*, 820–826.